Beam Adjustment with Double Subwavelength Metal Slits Surrounded by Tapered Dielectric Gratings

Beam Adjustment with Double Subwavelength Metal Slits Surrounded by Tapered Dielectric Gratings

ZOU Da-Qing(邹大庆), JIANG Jian-Li(蒋剑莉), LI Xiang-Yin(李相银)*

College of Science, Nanjing University of Science and Technology, Nanjing 210094

(Received 11 September 2009)

A beam optical focusing structure with double subwavelength metal slits surrounded by tapered surface dielectric gratings is proposed and demonstrated numerically. In the proposed structure, just with the regulation of the surface gratings, the radiation fields of surface plasmon polaritons (SPPs) can be controlled effectively to make a beam spot at several times the wavelength distance from the slit. Two methods for the control of focal length and width are proposed, and the simulation results verify that both the methods are effective for the design of nano-optical focusing devices.

PACS: 78. 20. Bh, 42. 79. Ag, 78. 20. −e DOI: 10.1088/0256-307X/27/1/017801

In conventional dielectric lenses forming an image of the dipole source,[1] a transmitted beam shows a strong diffraction effect at lens edges which becomes one of the limiting factors in scaling down conventional optics components to a wavelength or subwavelength range. Fortunately, the plasmonic lenses do not suffer from the edge effect and the beam focusing with nanometallic structures draws great interest for its potential realization of miniaturization of devices in subwavelength scale. Novel optical devices can be designed by introducing metallic structure due to the interactions with surface plasmons (SPs).[2−12] It is shown that appropriate design of simple metallic structures, such as slits, holes, and surface corrugations, can render flexible control of light.[13−19]

A metallic nanolens is designed in Ref. [2] to demonstrate beam shaping functions, which is based on the convex-shaped metallic nanoslit arrays resembling glasses lens in their shape. The principle and design approaches for designing flat nano-metallic surface palsmonic lens are given by Yuan *et al.*[3] Recently, a method for beam focusing by a single subwavelength metal slit surrounded by surface gratings has been proposed, the period of each surface grating is chirped so that the radiation fields of SPs can be controlled to make a beam spot at the desired focal length. In Ref. [5], the authors show that the relative phase of emitting light scattered by SP in a single subwavelength metallic groove can be modulated by the groove depth. These new findings extend the view of subwavelength imaging, and are very important to understand the underlying mechanism of plasmonic nanolens. Once we understand it, we can control the beaming of light beams in the microscopic world. Among these researches, various nano-optical research fields and technologies can be facilitated and amplified, such as the field of optical switches, optical sensor, optical lithography, optical storage, and optical microscopy, etc.[7]

In this Letter, a method for manipulating the beam through two subwavelength metal slits surrounded by tapered dielectric surface gratings is proposed based on the property that the direction of the radiation fields generated by SPPs can be changed by adjusting the form of the surface gratings. It was shown in Ref. [8] that the lensing ability is controlled by the output corrugation, whereas the transmissive properties are governed mainly by the input corrugation only. Here we put only the corrugation at the output side of the film. The SPP distributions and propagations are characterized by the method of two-dimensional finite-difference time-domain (2D-FDTD), with an anisotropic perfectly matched layer (APML) absorbing boundary conditions. From our method with numerical analysis, we can form the beam spot at the desired position and its full width at half maximum (FWHM) is slightly narrower than the wavelength of incident wave.

The basic concept of our proposed beam focusing method is shown in Fig. 1. The SPPs are excited from the metal slit and they propagate along each side on the metal silt. The lens is an Ag slab of thickness h with two subwavelength slits (whose widths are W_1 and W_2, respectively) surrounded by tapered dielectric gratings on the output side. The period of the grating is Λ, as shown in Fig. 1. The optical field is the p-polarized monochromatic wave with the wavelength of 532 nm in air. The dielectric function of Ag is described by the Drude model as follows:

$$\varepsilon_{A_g} = \varepsilon_\infty - \frac{\omega_p^2}{\omega(\omega + i\gamma)}, \tag{1}$$

where ε_∞ is the infinite frequency dielectric constant, ω_p the bulk plasma frequency, ω the angular frequency, and γ the collision frequency related to the dissipation loss in the metal. We assume

*Email: xyl@mail.njust.edu.cn

that the metal is silver ($\varepsilon_\infty = 3.7$, $\omega_p = 9\,\mathrm{eV}$ and $\gamma = 0.018\,\mathrm{eV}$).[17] We assume the monochromatic operation with the free space wave number $k_0 = \omega_0/c$, the time-dependency of $\exp(-j\omega t)$, and corresponding free space wave length $\lambda_0 = 2\pi/k_0$. Here c_0 is the speed of the light in vacuum. We consider the TM mode (p-polarized), so that H_x, E_y and H_z all are zero. A two-dimensional finite difference time domain (2D-FDTD) method has been used in this work. An anisotropic perfectly matched layer (APML) absorbing material is presented for the truncation of FDTD lattices for the simulation of electromagnetic fields.[18]

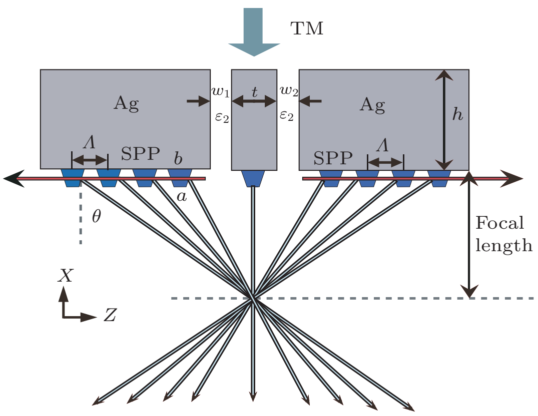

Fig. 1. Schematic diagram of the system studied: double subwavelength slits surrounded by tapered dielectric surface gratings on the output surface. A p-polarized EM plane wave is impinging from the top side. Here h denotes the thickness of the Ag film, t denotes the width of the middle Ag film, Λ denotes the period of the dielectric grating, a denotes the width of the dielectric grating, b denotes the thickness of the dielectric grating.

In our simulation, the refractive index, the fill factor of surface gratings are 1.72 and 0.5, respectively, the periods of gratings are 300 nm, the thickness of Ag film is 120 nm, the magnetic field intensity $|H_y|^2$ is used to represent the field intensity distributions in all the cases, b is fixed at 150 nm. The simulated field distribution of SPPs passing through the slit for $W_1 = W_2 = 50\,\mathrm{nm}$ is displayed in Fig. 2. The excited SPPs at each slit share the same phase, and the constructive interference of the SP waves emanating from different slits and surface gratings lead to an intense SPP focal spot. The important point of the result is that the focal length can be just several times of the wavelength.[5]

We can see that with increasing a, the focal length f, focal width δ (full width at half-maximum of field intensity along the x direction), and focal depth Δ (full width at half-maximum of field intensity along the z direction), all increase. The calculated results are presented in Table 1. The results are due to the modulating of the emissions' relative phase distribution on the output surface, which plays a crucial role in the interference of the light from gratings and slit.[6] The optical phase retardations can be made by designing of the surface grating to produce the desired focusing effect.

Table 1. The calculated focal length, focal width and depth with different a.

a (nm)	f (μm)	δ (μm)	Δ (nm)
60	1.79	0.761	397
90	1.895	1.059	452
120	2.055	1.376	506
150	2.34	1.748	548
180	2.415	1.982	612
210	2.865	2.274	700

In Ref. [6], the lensing ability is discussed by controlling the depth distribution of grooves. A phenomenon of focusing position shift is observed by employing a group of groove depths in curved distribution. Here a new method to make a beam spot at the desired focal length is proposed. In our model, we find that the depth distribution of surface dielectric gratings plays an important role in the beam focusing.

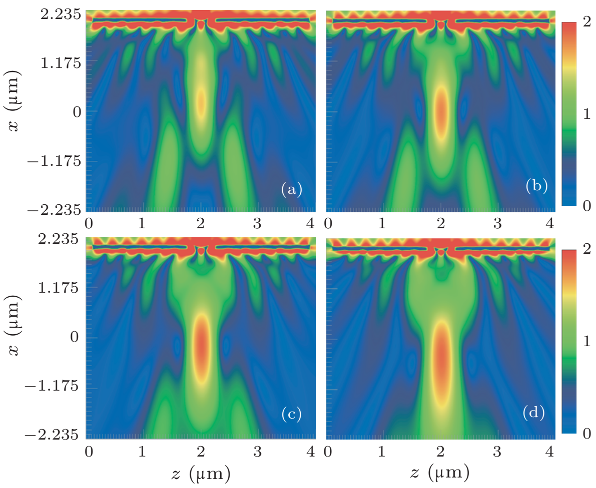

Fig. 2. Intensity distribution of the focused beam from two subwavelength metal slits with 11 surface gratings while $W_1 = W_2 = 50\,\mathrm{nm}$. Here b is fixed at 150 nm for (a) $a = 60$, (b) $a = 90$, (c) $a = 120$, (d) $a = 150\,\mathrm{nm}$.

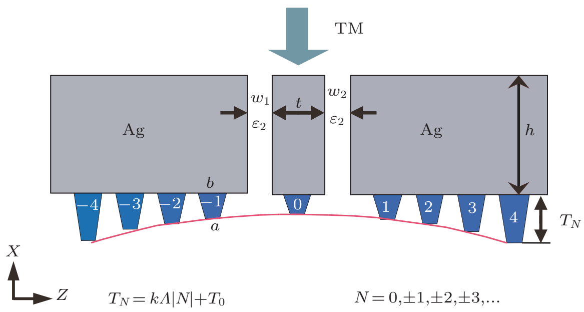

Fig. 3. Schematic view of the structures formed by double single subwavelength slits surrounded by tapered gratings with traced depth profile. T_N denotes the depth of grooves with the serial number of N; $k\Lambda$ denotes the depth difference between the adjacent gratings; and the other parameters are the same as those used in Fig. 1.

For the control structure, the depth of the central grating is set as T_0, while the modulated structure's groove depth spatially decreases or increases with the distance from the central slit, and for the linear case the depth trace can be defined as

$$T_N = k\Lambda|N| + T_0,\ N = 0, \pm1, \pm2, \ldots,$$

where T_N is the depth of grating with the serial number of N; $k\Lambda$ denotes the depth difference between the adjacent gratings; k is the degree of the depth trace tilted. In the following FDTD calculations, the wavelength and the silver dielectric constant are the same as those used in Fig. 2.

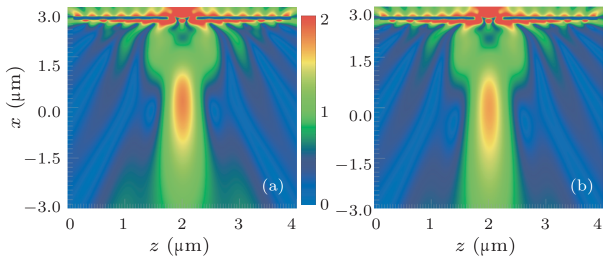

Fig. 4. Simulated intensity distributions of SPPs passing through the two subwavelength slits with 11 surface gratings for (a) $k\Lambda = 10$, (b) $k\Lambda = 20$ nm. The other parameters are the same as those used in Fig. 2.

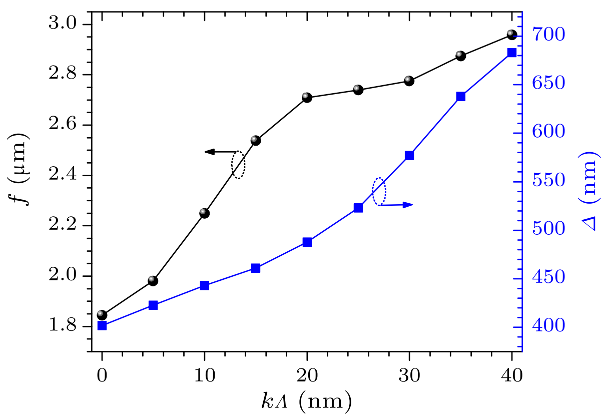

Fig. 5. Focal length and focal width versus $k\Lambda$. Here $k\Lambda$ increases from 0 to 40 nm with a step of 5 nm, and the other parameters are the same as those used in Fig. 4.

First we set $T_0 = 80$ nm, and consider the case $k\Lambda > 0$. Figures 4(a) and 4(b) illustrate the corresponding field intensity distributions for the case $k\Lambda = 10$ and $k\Lambda = 20$, respectively. The field intensity distribution results show that the energy emerging from the structure overlaps the axis within several microns, concentrating most of the energy in an extremely small region. For example, Fig. 4(a) reveals the focal length of 2.25 μm and the focal depth of 443 nm, i.e., focal spot smaller than a wavelength. More details of the dependence of focal length and width on grating depth trace profile are shown in Fig. 5. By increasing $k\Lambda$ from 0 to 40 nm at a step of 5 nm, the focal length increases steadily from 1.845 to 2.958 μm, and the FWHM of focal width increases steadily from 402 to 683 nm.

Then we set $T_o = 140$ nm, and consider the case $k\Lambda < 0$. Figures 6(a) and 6(b) illustrate the corresponding field intensity distributions for the case $k\Lambda = -10$ and $k\Lambda = -20$, respectively. We can see that the focal length is just several times of the wavelength. Figure 7 shows the details of the dependence of focal length and width on grating depth trace profile. This method is based on the radiation properties of SPPs which can be controlled by adjusting the surface gratings on the metal substrate.

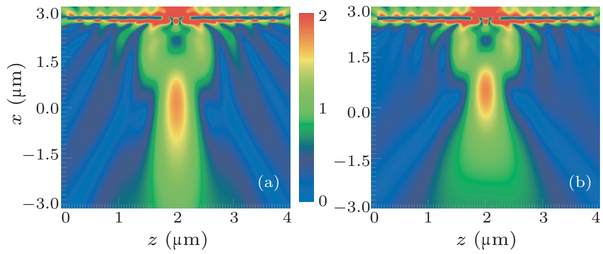

Fig. 6. Simulated intensity distributions of SPPs passing through the two subwavelength slits with 11 surface gratings for (a) $k\Lambda = -10$, (b) $k\Lambda = -20$ nm. The other parameters are the same as those used in Fig. 2.

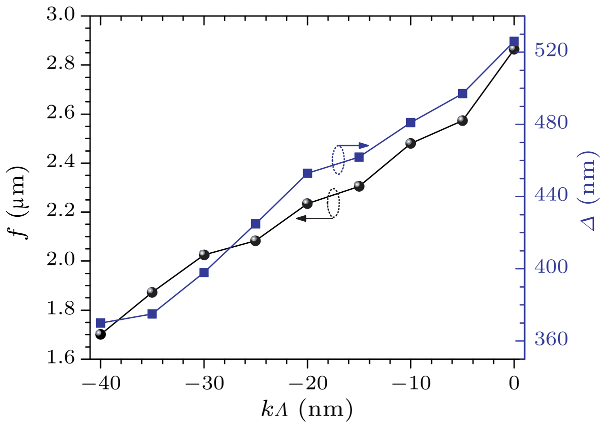

Fig. 7. Focal length and focal width versus with $k\Lambda$. Here $k\Lambda$ increases from -40 to 0 nm with a step of 5 nm, and the other parameters are the same as those used in Fig. 6.

In summary, we have proposed a beam focusing structure composed of double single subwavelength metal slits surrounded by tapered surface gratings, and we provide two methods for adjusting the focal length and width. Numerical simulation indicates that, like the structure with a single metal slit, the emissions' relative phase distribution profile of the structure with double subwavelength metal slits on the output surface can also be modulated by the surface gratings. Additional advantages of our methods discussed and demonstrated above are obvious. It is more effective for the structure with double slits to control focus length than the one with single slit. First, it can affect the field distribution in the back of the structure adjusting the two slits in turn. Secondly, the surface morphology of the two-slit structure affects the field distribution deeply, we can control the focal length of plasmonic lens by adjusting the surface gratings effectively. It is concluded that we can make a beam spot which is located at several times the wavelength distance from the slit, and its focal length can be controlled. The high focusing performance of the proposed structures may be used in data storage devices, bioimaging, and nanolithography.

The authors would like to thank QIN Zi-Jian and WU Hong for their kind contribution to this work.

References

[1] Born M and Wolf E 1999 *Principles of Optics* 7th edn (Cambridge: Cambridge University) chap 8 p 412
[2] Sun Z and Kim H K 2004 *Appl. Phys. Lett.* **85** 642
[3] Yuan H X, Xu B X, Lukiyanchuk B and Chong T C 2007 *Appl. Phys.* A **89** 397
[4] Sun Z 2006 *Appl. Phys. Lett.* **89** 261119
[5] Kim S, Lim Y, Kim H, Park J and Lee B 2008 *Appl. Phys. Lett.* **92** 013103
[6] Shi H F, Du C L and Luo X G 2007 *Appl. Phys. Lett.* **91** 093111
[7] Yu L B, Lin D Z, Chang Y C and Huang K T 2005 *Phys. Rev.* B **71** 041405(R)
[8] Garcia-Vidal F J, Martin-Moreno L, Lezec H J and Ebbesen T W 2003 *Appl. Phys. Lett.* **83** 4500
[9] Wang Q, Yuan X C, Tan P and Zhang D G 2008 *Opt. Express* **16** 19271
[10] Shi H F, Wang C T, Du C L, Luo X G, Dong X C and Gao H T 2005 *Opt. Express* **13** 6815
[11] Lee K L, Lee Ch W, Wei P K 2007 *Appl. Phys. Lett.* **90** 233119
[12] Zheng G G and Li X Y 2009 *J. Opt. A: Pure Appl. Opt.* **11** 075002
[13] Mário G, Silveirinha, Belov P A and Simovski C R 2008 *Opt. Lett.* **33** 1726
[14] Min C J, Wang P, Jiao X J, Deng Y and Ming H 2007 *Opt. Express* **15** 9541
[15] Kim S, Kim H, Lim Y and Lee B 2007 *Appl. Phys. Lett.* **90** 051113
[16] Wang Ch T, DU Ch L, Lv Y G and Luo X G 2006 *Opt. Express* **14** 5671
[17] Park J, Kim H and Lee B 2008 *Opt. Express* **16** 413
[18] Gedney S D 1996 *IEEE Trans. Antennas Propag.* **44** 1630
[19] Yang X Y, Xie W Ch and Liu D M 2008 *Chin. Phys. Lett.* **25** 148